
Enabling wave-based inversion on GPUs with randomized trace estimation

Mathias Louboutin¹, Felix J. Herrmann^{1,2}

¹ School of Earth and Atmospheric Sciences, Georgia Institute of Technology

² School of Computational Science and Engineering, Georgia Institute of Technology

1 Summary

By building on recent advances in the use of randomized trace estimation to drastically reduce the memory footprint of adjoint-state methods, we present and validate an imaging approach that can be executed exclusively on accelerators. Results obtained on field-realistic synthetic datasets, which include salt and anisotropy, show that our method produces high-fidelity images. These findings open the enticing perspective of 3D wave-based inversion technology with a memory footprint that matches the hardware and that runs exclusively on clusters of GPUs without the undesirable need to offload certain tasks to CPUs.

2 Introduction

Subsurface imaging has recently thrived building on advances in wave-equation based methods such as Full-Waveform Inversion (FWI) and Reverse-Time Migration (RTM) [1, 2]. However, these methods rely on extremely high computational and memory costs, which explains the relative limited widespread adaptation of these technologies. Unfortunately, exceedingly large memory footprints are inherent to the adjoint-state method [1, 3], which requires storage (in memory, on disk, possibly compressed) of the complete time history of the forward modeled wavefield in order to compute the imaging condition that correlates this forward wavefield with the time-reversed solution of the adjoint wave equation. Because saving forward modeled wavefields requires terabytes of memory for industry scale high-frequency 3D imaging, memory usage has been and continues to be a major bottleneck on standard with the exception perhaps of dedicated high-memory nodes available in the cloud. While dedicated nodes relieve some of the memory pressure, they do not allow use of accelerators to speed up computations. Contrary to conventional computer hardware, memory on accelerators comes at a premium, which is problematic given the large memory footprint of adjoint-state methods. To address this problem, several methods have been proposed over the years where excessive memory footprints are offset by incurring computational overhead. A good example of such an approach is the method of optimal checkpointing proposed by Griewank and Walther [4] and Symes [5]. This method was initially introduced to tackle memory limitation of CPUs and has been used successfully in 3D seismic applications. To further limit the computational overhead, Kukreja et al. [6] recently supplemented this approach by adding on-the-fly compression and decompression of the forward wavefields. In situations where the wave physics is reversible, researchers [7–9] have shown that forward wavefields can also be recomputed from boundary values. Unfortunately, both approaches are challenged by underlying assumptions. They also require a relative high of algorithmic complexity. This explains why GPUS-native implementations of adjoint-state methods including on-the-fly compression remain illusive.

While recomputing forward wavefields as part of memory-footprint mitigation certainly has its merits, there exist simpler randomized approaches where memory use is traded against computational overhead and controllable error. Unlike approaches that aim to compute gradients exactly, these methods approximate the gradient with the aim to reduced computational and memory costs at the expense of a controllable loss in accuracy. Examples of such an approach include to working with

random subsets of shots [10] or simultaneous shots [11–15], or with randomized singular value decompositions [16, 17] and random-trace estimation. The latter was used by Haber et al. [14] to analyze computational speedups of full-waveform with computational simultaneous sources. As long as the errors are controlled, these methods lead to equivalent inversion results at fraction of the computational costs (e.g. speedups of a factors of seven have been reported for FWI [18]). Following ideas from randomized linear algebra to estimate the trace of a matrix, Louboutin and Herrmann [19] proposed an approximation of the adjoint-state method that leads to major memory improvements and is relatively easy to implement and supported by theory [20, 21], guaranteeing convergence including bounds on the accuracy. However, unlike other approximate methods, such as on-the-fly Fourier-based [22] or lossy compression-based algorithms [6], the artifacts introduced by the proposed randomized trace estimation are incoherent and appear as Gaussian-like noise, which can be handled easily by sparsity-promoting imaging [22]. While the initial results of the randomized trace estimation on a simple 2D synthetic were encouraging [19], we submit the proposed approximation to additional scrutiny by considering complex imaging examples that involve salt (SEAM model [23]) and anisotropy [24] (BP TTI model).

Our contributions are organized as follows. First, we briefly introduce randomized trace estimation and its computational benefits during RTM and the formation of horizontal subsurface-offset image volumes [25]. Next, we show its application to two representative examples, long-offset subsalt imaging on the 2D SEAM acoustic model with a sparse ocean-bottom node acquisition, and TTI anisotropic imaging of the 2D BP TTI model. With these examples, we validate the computational efficiency and practicality of our method on GPUs available on Azure (the Standard_NC6 virtual machine).

3 Methodology

Before we demonstrate the advocacy of the proposed methodology on complex imaging problems, let us first quickly discuss how randomized trace estimation can be used to reduce the memory footprint of adjoint-state wave-based seismic imaging. We do this by showing that applying the imaging condition corresponds to computing the trace of a matrix.

3.1 Randomized trace estimation

Approximating [Avron; 21] the identity \mathbf{I} by

$$\text{tr}(\mathbf{A}) = \text{tr}(\mathbf{A}\mathbb{E}[\mathbf{z}\mathbf{z}^\top]) = \mathbb{E}[\text{tr}(\mathbf{A}\mathbf{z}\mathbf{z}^\top)] = \mathbb{E}[\mathbf{z}^\top\mathbf{A}\mathbf{z}] \approx \frac{1}{r} \sum_{i=1}^r [\mathbf{z}_i^\top\mathbf{A}\mathbf{z}_i] = \frac{1}{r} \text{tr}(\mathbf{Z}^\top\mathbf{A}\mathbf{Z}) \quad (1)$$

lies at the heart of randomized trace estimation where the \mathbf{z}_i 's are random probing vectors for which $\mathbb{E}(\mathbf{z}^\top\mathbf{z}) = 1$ with \mathbb{E} is the stochastic expectation operator. This above estimator for the trace (sum of the diagonal of the matrix \mathbf{A} , $\text{tr}(\mathbf{A}) = \sum_i \mathbf{A}_{ii}$) is unbiased (i.e., exact in expectation) and converges to the true trace with an error that decays with r and without access to the entries of \mathbf{A} . Only actions of \mathbf{A} on the probing vectors are needed and we exploit this property and the specific structure of the matrix \mathbf{A} in gradient calculations for wave-equation based inversion. Motivated by recent work [21, 26] we also employ a partial qr factorization [27] that approximates the range of the matrix \mathbf{A} —i.e., we approximate the trace with probing vectors $[\mathbf{Q}, \sim] = \text{qr}(\mathbf{A}\mathbf{Z})$ where \mathbf{Z} is a Rademacher random matrix of ± 1 .

3.2 Approximate gradient calculations

While the presented randomized approach carries over to arbitrary complex wave physics, we derive our memory reduced gradient approximation for the isotropic acoustic case where the gradient for a single source $\delta\mathbf{m}$ can be written as

$$\delta\mathbf{m} = \sum_{t=1}^{n_t} \ddot{\mathbf{u}}[t]\mathbf{v}[t]. \quad (2)$$

In this expression, $\mathbf{u}[t], \mathbf{v}[t]$ are the vectorized (along space) full-space forward and adjoint wavefields at time index $t = 1 \cdots n_t$ with n_t the number of timesteps. The symbol $\ddot{\cdot}$ represents second-order time derivative. To arrive at a form where randomized trace estimation can be used, we write the

above zero-lag imaging condition over time as the trace of the outer product for each space index \mathbf{x} separately. By using the dot product property, $\sum x_i y_i = \mathbf{x}^\top \mathbf{y} = \text{tr}(\mathbf{x}\mathbf{y}^\top)$, and the approximation in Equation 1, the gradient at location \mathbf{x} becomes

$$\delta \mathbf{m}[\mathbf{x}] = \text{tr}(\ddot{\mathbf{u}}[\cdot, \mathbf{x}]\mathbf{v}[\cdot, \mathbf{x}]^\top) \approx \frac{1}{r} \text{tr}(\bar{\mathbf{u}}[\cdot, \mathbf{x}]\bar{\mathbf{v}}[\cdot, \mathbf{x}]^\top) \quad \text{with} \quad \bar{\mathbf{u}} = \mathbf{Q}^\top \ddot{\mathbf{u}}, \bar{\mathbf{v}} = \mathbf{Q}^\top \mathbf{v}. \quad (3)$$

Contrary to the sum over all timesteps t , the zero-offset imaging condition in Equation 3 involves storage of the compressed wavefields for only $r \ll n_t$ timesteps. This compression not only significantly reduces the memory footprint but it also lessens the computational cost of computing imaging conditions as a function of the horizontal subsurface offset

$$\delta \mathcal{M}[\mathbf{x}, \mathbf{h}] \approx \frac{1}{r} \text{tr}(\bar{\mathbf{u}}[\cdot, \mathbf{x} + \mathbf{h}]\bar{\mathbf{v}}[\cdot, \mathbf{x} - \mathbf{h}]^\top) \quad (4)$$

with \mathbf{h} the horizontal subsurface offset and $\delta \mathcal{M}[\mathbf{h}]$ the subsurface image volume. As with computing the zero-offset imaging condition in Equation 3, the cost of computing these volumes is also reduced by a factors of r/n_t . Also notice that $\delta \mathbf{m}[\mathbf{x}] = \delta \mathcal{M}[\mathbf{x}, \mathbf{h}]|_{\mathbf{h}=\mathbf{0}}$.

Figure 1 contains subsurface offset gathers for the 2007 BP TTI model discussed in more detail below. Despite the fact that we used only a limited ($r = 64 \ll n_t$) probing factors, the images gathers are properly focused around and nearly noise free thanks to the noise stacking. Each image volume is using 81 offsets ($-500\text{m} : 12.5\text{m} : 500\text{m}$) and is effectively using more memory that we needed to store the compressed wavefields needed to compute these volumes, highlighting how memory frugal the proposed trace estimation method really is.

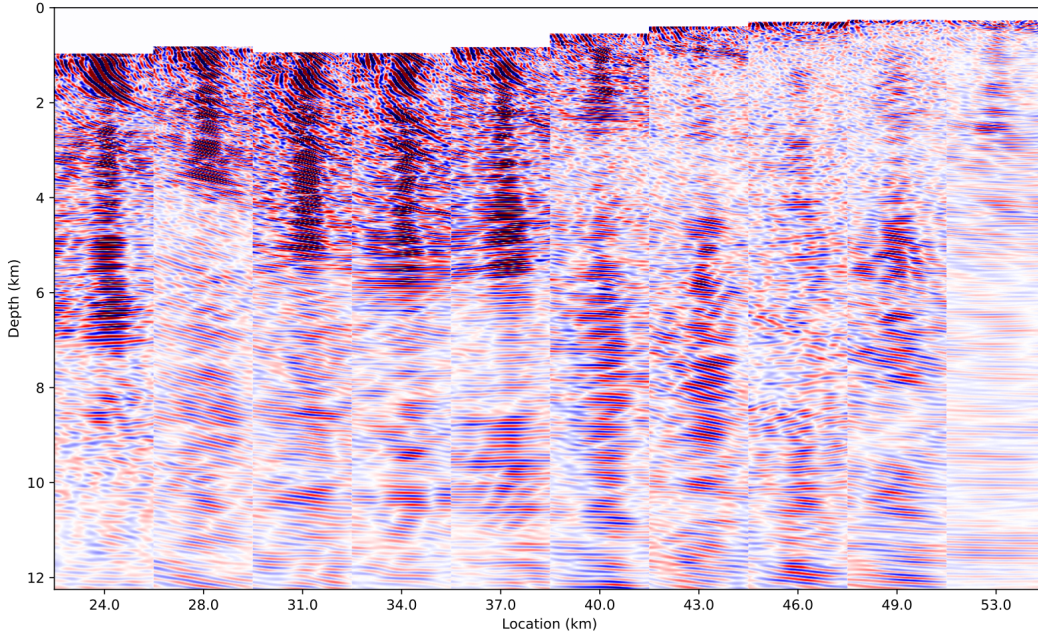


Figure 1: Subsurface offset gathers with a -500m to 500m horizontal offset.

4 Synthetic case studies

To validate the proposed technology, we consider the 2D acoustic SEAM model and the 2D 2007 BP TTI model. We chose these models because they are complex and in need of a large number of timesteps. As the examples included below, we obtain reasonable RTM images for a limited number of probing vectors ($r = 64$), yielding a memory reduction by a factor of $100\times$ — $150\times$ reducing the memory footprint to less than 2Gb. This drastic memory reduction allows us to fully take advantage of accelerators by performing the RTM imaging natively on GPUs without relying on advanced IO or checkpointing techniques. More details on memory gains are included in Table 1. We refer to [19] for more details on memory cost and computational overhead of the proposed method.

	Standard RTM	Trace Estimation	Gain (\times)
SEAM	380/94 Gb	1.4/.7 Gb	271–134
BP TTI	337/75 Gb	2.1/1.05 Gb	160–71

Table 1: Memory usage of standard adjoint-state RTM (full history/sampled at 4ms) versus imaging via random trace estimation with $r = 64/32$ on the 2D SEAM model and 2D BP TTI model.

4.1 2D SEAM model

To study the behavior of our approximation on long-offset sparse OBN acquisition, we consider a 2D slice of the SEAM salt model [23]. Because this type of acquisition improves the illumination of large salt bodies in the Gulf of Mexico, this type of acquisition has recently gained in popularity. The survey consists of 44 OBNs one kilometer apart. At the surface, sources are located every 12.5m at a depth of 12.5m. We idealized this dataset by modeling with reciprocity, which leads to 44 densely sampled common receiver gathers that serve as input to our approximate imaging approach. As we can clearly see from Figure 2, we are able to produce a good image despite complexity of the model and drastic compression of the wavefield (we use only $r = 64$ probing vectors. Even though we incur limited noise mostly in shallow areas, we argue that these noisy artifacts can easily be removed. At greater depth, the imprint of the noise is less leading to good resolution below the salt.

4.2 2007 BP TTI

To demonstrate that the proposed method can be extended to more complex imaging physics, we also included an anisotropic example where a subset of the 2007 BP TTI dataset is imaged. Figure 3 includes the imaging result. From this image, we observe that all the layers are imaged correctly and continuously. Because we have a much denser acquisition in this case, the noise incurred by the randomized trace estimation mostly stacks out leading to a very clean image for a fraction of the memory cost of standard RTM. Again all calculations were done exclusively on the GPU.

4.3 Code availability

Our implementation and examples are available as open-source software at [TimeProbeSeismic.jl](#), which extends our Julia inversion framework [JUDI.jl](#)[28]. Our code is also designed to generalize to 3D and more complicated physics as supported by [Devito](#)[29, 30].

5 Discussion and conclusions

We presented a proof of concept of wave-based seismic inversion with randomized trace estimation. Aside from demonstrating that this method leads to drastic memory reductions that allow us to form subsurface-offset gathers while remaining on the GPU, we also showed that the incoherent imaging artifacts mostly stack out. This allowed us to create high fidelity images for realistic anisotropic models with salt. Unlike existing methods based on on-the-fly Fourier transforms, we observed that imaging artifacts induced by the random trace estimation stack out for a high enough fold. We expect that this reliance on fold can be relaxed when carrying sparsity-promoting imaging or full-waveform inversion with constraints. More importantly, the drastic memory reduction allows us to carry out the imaging exclusively on GPUs.

6 Acknowledgement

This research was carried out with the support of Georgia Research Alliance and partners of the ML4Seismic Center.

References

- [1] Albert Tarantola. Inversion of seismic reflection data in the acoustic approximation. *GEO-PHYSICS*, 49(8):1259, 1984. doi: 10.1190/1.1441754. URL [+http://dx.doi.org/10.1190/1.1441754](http://dx.doi.org/10.1190/1.1441754).

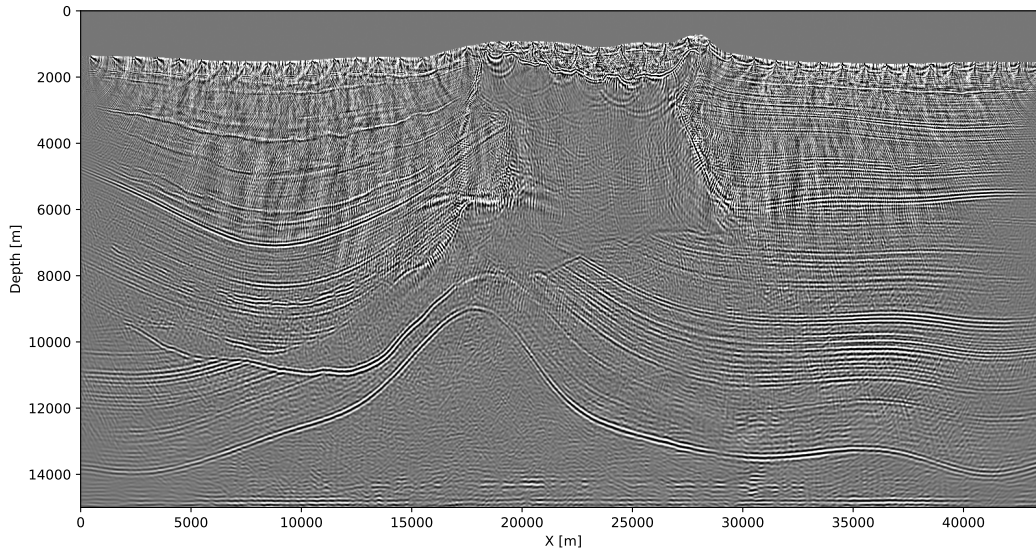


Figure 2: 2D RTM on the SEAM model with sparse OBN acquisition.

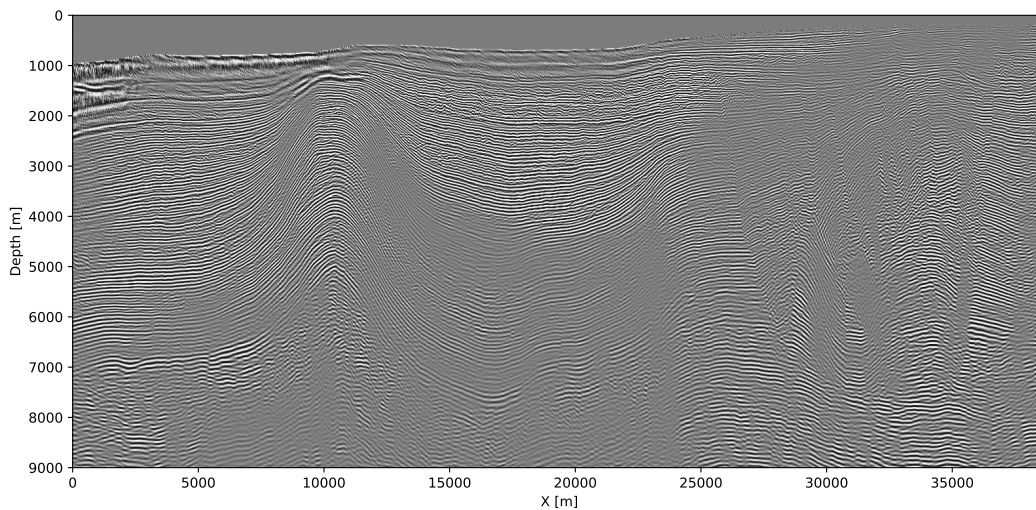


Figure 3: 2D RTM on the 2007 BP TTI model with a marine acquisition.

1441754.

- [2] J. Virieux and S. Operto. An overview of full-waveform inversion in exploration geophysics. *GEOPHYSICS*, 74(5):WCC1–WCC26, 2009. doi: 10.1190/1.3238367. URL <http://library.seg.org/doi/abs/10.1190/1.3238367>.
- [3] J. L. Lions. *Optimal control of systems governed by partial differential equations*. Springer-Verlag Berlin Heidelberg, 1st edition, 1971. ISBN 978-3-642-65026-0.
- [4] Andreas Griewank and Andrea Walther. Algorithm 799: Revolve: An implementation of checkpointing for the reverse or adjoint mode of computational differentiation. *ACM Trans. Math. Softw.*, 26(1):19–45, March 2000. ISSN 0098-3500. doi: 10.1145/347837.347846. URL <http://doi.acm.org/10.1145/347837.347846>.
- [5] Symes. Reverse time migration with optimal checkpointing. *GEOPHYSICS*, 72(5):SM213–SM221, 2007. doi: 10.1190/1.2742686. URL <http://library.seg.org/doi/abs/10.1190/1.2742686>.

- [6] N. Kukreja, J. Hükelheim, M. Louboutin, J. Washbourne, P. H. J. Kelly, and G. J. Gorman. Lossy checkpoint compression in full waveform inversion. *Geoscientific Model Development Discussions*, 2020:1–26, 2020. doi: 10.5194/gmd-2020-325. URL <https://gmd.copernicus.org/preprints/gmd-2020-325/>.
- [7] G. A. McMechan. Migration by extrapolation of time-dependent boundary values. *Geophysical Prospecting*, 31(3):413–420, 1983. ISSN 1365-2478. doi: 10.1111/j.1365-2478.1983.tb01060.x. URL <http://dx.doi.org/10.1111/j.1365-2478.1983.tb01060.x>.
- [8] Rune Mittet. Implementation of the kirchhoff integral for elastic waves in staggered-grid modeling schemes. *GEOPHYSICS*, 59(12):1894–1901, 1994. doi: 10.1190/1.1443576. URL <http://dx.doi.org/10.1190/1.1443576>.
- [9] Espen Birger Raknes and Wiktor Weibull. Efficient 3d elastic full-waveform inversion using wavefield reconstruction methods. *Geophysics*, 81(2):R45–R55, 2016. ISSN 0016-8033. doi: 10.1190/geo2015-0185.1. URL <http://geophysics.geoscienceworld.org/content/81/2/R45>.
- [10] Michael P. Friedlander and Mark Schmidt. Hybrid deterministic-stochastic methods for data fitting. *SIAM Journal on Scientific Computing*, 34(3):A1380–A1405, 2012. doi: 10.1137/110830629. URL <https://doi.org/10.1137/110830629>.
- [11] Louis A. Romero, Dennis C. Ghiglia, Curtis C. Ober, and Scott A. Morton. Phase encoding of shot records in prestack migration. *GEOPHYSICS*, 65(2):426–436, 2000. doi: 10.1190/1.1444737. URL <https://doi.org/10.1190/1.1444737>.
- [12] Jerome R. Krebs, John E. Anderson, David Hinkley, Ramesh Neelamani, Sunwoong Lee, Anatoly Baumstein, and Martin-Daniel Lacasse. Fast full-wavefield seismic inversion using encoded sources. *GEOPHYSICS*, 74(6):WCC177–WCC188, 2009. doi: 10.1190/1.3230502. URL <https://doi.org/10.1190/1.3230502>.
- [13] Peyman P. Moghaddam, Henk Keers, Felix J. Herrmann, and Wim A. Mulder. A new optimization approach for source-encoding full-waveform inversion. *GEOPHYSICS*, 78(3):R125–R132, 2013. doi: 10.1190/geo2012-0090.1. URL <https://doi.org/10.1190/geo2012-0090.1>.
- [14] Eldad Haber, Kees van den Doel, and Lior Horesh. Optimal design of simultaneous source encoding. *Inverse Problems in Science and Engineering*, 23(5):780–797, 2015. doi: 10.1080/17415977.2014.934821. URL <https://doi.org/10.1080/17415977.2014.934821>.
- [15] Tristan van Leeuwen and Felix J. Herrmann. Fast waveform inversion without source-encoding. *Geophysical Prospecting*, 61(s1):10–19, 2013. doi: <https://doi.org/10.1111/j.1365-2478.2012.01096.x>. URL <https://onlinelibrary.wiley.com/doi/abs/10.1111/j.1365-2478.2012.01096.x>.
- [16] Tristan van Leeuwen, Rajiv Kumar, and Felix J. Herrmann. Enabling affordable omnidirectional subsurface extended image volumes via probing. *Geophysical Prospecting*, 65(2):385–406, 03 2017. doi: 10.1111/1365-2478.12418. URL <https://slim.gatech.edu/Publications/Public/Journals/GeophysicalProspecting/2016/vanleeuwen2015GPWEMVA/vanleeuwen2015GPWEMVA.pdf>. (Geophysical Prospecting).
- [17] Mengmeng Yang, Marie Graff, Rajiv Kumar, and Felix J. Herrmann. Low-rank representation of omnidirectional subsurface extended image volumes. *Geophysics*, 86(3):1–41, 1 2021. doi: 10.1190/geo2020-0152.1. URL https://slim.gatech.edu/Publications/Public/Journals/Geophysics/2021/yang2020lrpo/Paper_final.html. (Geophysics).
- [18] Jerome R. Krebs, John E. Anderson, David Hinkley, Anatoly Baumstein, Sunwoong Lee, Ramesh Neelamani, and Martin-Daniel Lacasse. *Fast full wave seismic inversion using source encoding*, pages 2273–2277. 2009. doi: 10.1190/1.3255314. URL <https://library.seg.org/doi/abs/10.1190/1.3255314>.
- [19] Mathias Louboutin and Felix J. Herrmann. Ultra-low memory seismic inversion with randomized trace estimation. In *SEG Technical Program Expanded Abstracts*, pages 787–791, 09 2021. doi: 10.1190/segam2021-3584072.1. URL <https://slim.gatech.edu/Publications/Public/Conferences/SEG/2021/louboutin2021SEGulm/louboutinp.html>. (IMAGE, Denver).

- [20] Haim Avron and Sivan Toledo. Randomized algorithms for estimating the trace of an implicit symmetric positive semi-definite matrix. *J. ACM*, 58(2), April 2011. ISSN 0004-5411. doi: 10.1145/1944345.1944349. URL <https://doi.org/10.1145/1944345.1944349>.
- [21] Raphael A. Meyer, Cameron Musco, Christopher Musco, and David P. Woodruff. Hutch++: Optimal Stochastic Trace Estimation. *arXiv e-prints*, art. arXiv:2010.09649, October 2020.
- [22] Philipp A. Witte, Mathias Louboutin, Fabio Luporini, Gerard J. Gorman, and Felix J. Herrmann. Compressive least-squares migration with on-the-fly fourier transforms. *Geophysics*, 84(5): R655–R672, 08 2019. doi: 10.1190/geo2018-0490.1. URL <https://slim.gatech.edu/Publications/Public/Journals/Geophysics/2019/witte2018cls/witte2018cls.pdf>. (Geophysics).
- [23] Michael Fehler and P. Joseph Keliher. *SEAM Phase I: Challenges of Subsalt Imaging in Tertiary Basins, with Emphasis on Deepwater Gulf of Mexico*. Society of Exploration Geophysicists, 01 2011. ISBN 9781560802877. doi: 10.1190/1.9781560802945. URL <https://doi.org/10.1190/1.9781560802945>.
- [24] Leon Thomsen. Weak elastic anisotropy. *Geophysics*, 51(10):1964–1966, 1986.
- [25] William W. Symes. Migration velocity analysis and waveform inversion. *Geophysical Prospecting*, 56(6):765–790, 2008. doi: <https://doi.org/10.1111/j.1365-2478.2008.00698.x>. URL <https://onlinelibrary.wiley.com/doi/abs/10.1111/j.1365-2478.2008.00698.x>.
- [26] Marie Graff-Kray, Rajiv Kumar, and Felix J. Herrmann. Low-rank representation of omnidirectional subsurface extended image volumes, 2017. URL <https://slim.gatech.edu/Publications/Public/Conferences/SINBAD/2017/Fall/graff2017SINBADFlrp/graff2017SINBADFlrp.pdf>.
- [27] Lloyd N Trefethen and David Bau III. *Numerical linear algebra*. Siam, 1st edition, 1997.
- [28] Philipp A. Witte, Mathias Louboutin, Navjot Kukreja, Fabio Luporini, Michael Lange, Gerard J. Gorman, and Felix J. Herrmann. A large-scale framework for symbolic implementations of seismic inversion algorithms in julia. *GEOPHYSICS*, 84(3):F57–F71, 2019. doi: 10.1190/geo2018-0174.1. URL <https://doi.org/10.1190/geo2018-0174.1>.
- [29] M. Louboutin, M. Lange, F. Luporini, N. Kukreja, P. A. Witte, F. J. Herrmann, P. Velesko, and G. J. Gorman. Devito (v3.1.0): an embedded domain-specific language for finite differences and geophysical exploration. *Geoscientific Model Development*, 12(3):1165–1187, 2019. doi: 10.5194/gmd-12-1165-2019. URL <https://www.geosci-model-dev.net/12/1165/2019/>.
- [30] Fabio Luporini, Mathias Louboutin, Michael Lange, Navjot Kukreja, Philipp Witte, Jan Hückelheim, Charles Yount, Paul H. J. Kelly, Felix J. Herrmann, and Gerard J. Gorman. Architecture and performance of devito, a system for automated stencil computation. *ACM Trans. Math. Softw.*, 46(1), April 2020. ISSN 0098-3500. doi: 10.1145/3374916. URL <https://doi.org/10.1145/3374916>.